

A study of single-wall carbon nanotubes using Renishaw's structural and chemical analyser for scanning electron microscopy

Overview

Electron imaging and Raman spectroscopy are established techniques for viewing and analysing carbon nanotubes. Performing these two techniques usually requires the sample being transferred between a scanning electron microscope (SEM) and a Raman spectrometer. This application note illustrates the advantages of Renishaw's structural and chemical analyser (SCA) for simultaneous secondary electron imaging and Raman spectroscopy of single-wall carbon nanotubes (SWNTs).

Introduction

Since their first observation by Sumio Iijima in 1991,¹ carbon nanotubes have attracted intense scientific interest due to their extraordinary electronic, thermal, and mechanical properties. The structure can be visualised as a graphite layer rolled up into a seamless cylinder, with each end either open or capped with half a fullerene molecule. The points at which the rolled up graphite sheet are connected define the tube's diameter and chirality, which, in turn, govern its properties.

Most current research is focused on SWNTs as they have superior electrical, thermal, and mechanical properties to their earlier discovered multi-wall counterparts (made up of concentric tubes). Ten times stronger than steel, and six times lighter, SWNT composite materials are expected to find numerous engineering uses; for example reducing spacecraft weight by at least 50%. Depending on their diameter and chirality, SWNTs can show metallic or semiconducting electrical behaviour, with applications as nanoscale wires and electrical components, whilst their high thermal conductivity (as high as diamond), makes them useful candidates for a range sensor and other applications.

Raman spectroscopy is one of the key analytical techniques for characterising SWNTs. Raman spectra are used to determine tube diameter, chirality, electronic properties, and strain, in both bulk and isolated nanotube samples.²⁻⁶ In addition, the alignment of carbon nanotubes within composite materials can be determined by Raman spectroscopy.⁷ Interest in the Raman analysis of isolated SWNTs has grown since the discovery in 2002 that isolated nanotubes exhibit resonant Raman behaviour, which provides detailed information about the electronic structure.⁴ This note

describes the use of Renishaw's SCA for the rapid location and Raman analysis of isolated SWNTs.

Raman spectroscopy of SWNTs

The main features in the Raman spectra of carbon nanotubes are: the radial breathing mode (RBM), which is a totally symmetric (in the ring plane) vibrational mode with A symmetry; the disorder-induced D-band, also with A symmetry, and its corresponding second-order G'-band; and the tangential G-band, which is made up of a mixture of symmetric and asymmetric in-plane modes (A and E₁ symmetry), and asymmetric out-of-plane modes (E₂ symmetry). For a detailed explanation of the symmetry properties refer to Reference 6.

Carbon nanotubes often form as an entangled mass of ropes or bundles and, since the frequency of the RBM (usually in the region 150 cm⁻¹ to 300 cm⁻¹) depends directly on tube diameter, resonance Raman spectra of this mode are used to provide an easy and quick determination of the tube diameter distribution in a sample.^{2,6,8} The fine structure seen in the tangential G-band depends on tube diameter and chirality, and the most intense diameter-dependent feature (around 1590 cm⁻¹) can be used (in conjunction with the RBMs) to help identify individual metallic and semiconducting SWNTs.² The G-band is also affected by the oxidation state of the nanotubes,⁵ and has been used to measure strain in SWNTs embedded in a matrix.³ The frequency of the disorder-

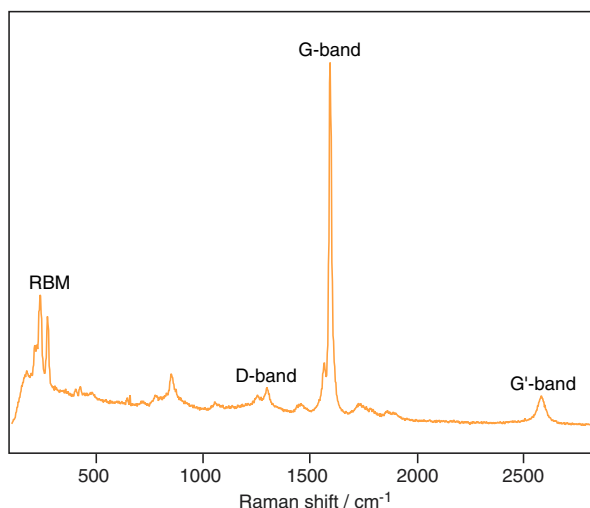


Figure 1
Typical Raman spectrum of bulk SWNTs using 785 nm excitation

induced D-band depends on nanotube diameter *and* chirality, making it strongly dependent on the electronic structure. The G'-band is the second-order overtone of the D-band, and, unlike the D-band, its intensity is not reduced in highly ordered crystals. Therefore the G'-band is used to provide electronic structural information on isolated SWNTs.⁴

For laboratory Raman applications, micro-sampling is usually achieved with a research grade optical microscope, which enables both sample viewing, and light delivery and collection.

Raman spectra of bulk SWNTs can be acquired easily and rapidly using a Renishaw Raman microscope (see Figure 1 for a typical Raman spectrum acquired using 785 nm laser excitation). Raman microscopy of isolated SWNTs is more difficult, since the optical microscope has insufficient spatial resolution to discriminate discrete nanotubes. Raman analysis of isolated SWNTs has been achieved in the past with a Renishaw Raman microscope by scanning a low-density SWNT sample with the laser spot in 0.5 μm steps using a controlled microscope xy stage until a characteristic SWNT Raman signal is observed, indicating that an SWNT has been

located.⁴ Although this technique is successful, location of isolated nanotubes in this way can be a time-consuming operation.

The structural and chemical analyser

The SCA is fitted to the SEM column and provides the interface between the SEM and Raman spectrometer. It comprises a retraction mechanism, collection optics, and a compact fibre optic video probe, and is available in two variants: a fully bakeable manual system (Fig. 2) for studies of clean surfaces in an ultra-high vacuum (UHV), as used in this study; and a high vacuum version (Fig. 3) that can be coupled to most makes and models of SEM. Both versions provide the means for performing Raman spectroscopy simultaneously with secondary electron imaging (the principal SEM imaging mode), without compromising the SEM performance in any way. The SCA collection optics are also fully compatible with both photoluminescence and cathodoluminescence spectroscopies, so the electrical and physical properties of samples can also be probed at the sub-micrometer scale.

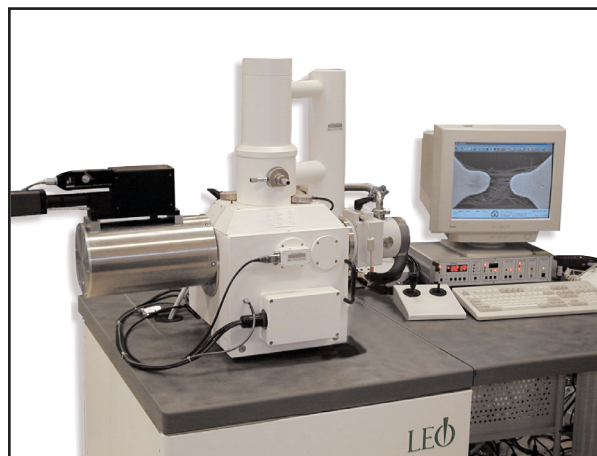


Figure 2
UHV-version of the structural and chemical analyser interface coupled to a LEO-1450VP SEM

The high spatial resolution afforded by SEM techniques (typically 3 to 4 orders of magnitude better than optical microscopy) allows the collection of images from sub-micrometre structures not observable with optical microscopy. Sensitive SEM contrast mechanisms also enable optically identical or similar materials to be distinguished easily, and, in combination with the high depth of field, make SEM an ideal technique for viewing isolated SWNTs.

Most SEMs are routinely fitted with energy dispersive spectroscopy (EDS) equipment, an x-ray emission technique used for microanalysis. However, EDS is unsuitable for samples such as carbon nanotubes since it provides only elemental information, has poor sensitivity to light elements, and very little of the x-ray spectrum is generated from the surface. The success of Raman spectroscopy for characterising carbon nanotubes, however, is well-documented, as described above.



Figure 3
High vacuum version of the structural and chemical analyser interface coupled to a JEOL SEM

Renishaw's structural and chemical analyser combines the resolving and visualising power of SEM with the chemical and physical identification power of Raman spectroscopy, enabling users to locate samples with the SEM and characterise their chemical and structural properties with Raman, without having to move the sample or collection optics.

Experimental

In this study, the ultra high vacuum (UHV) version of the structural and chemical analyser was used, fitted to a LEO-1450VP SEM (Fig. 2).

The SCA enables observation of the spectroscopic analysis area as a micrometre-scale spot projected onto the sample surface in the SEM image. The fibre optic output from the

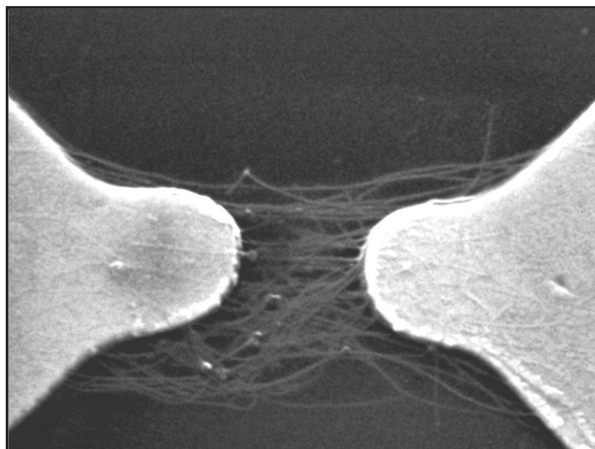


Figure 4
SEM image of nanotubes aligned between two electrodes

SCA was connected to a Renishaw RM1000 spectrometer unit for spectral analysis, equipped with 532 nm and 633 nm laser excitation.

Two samples were analysed: a bulk sample consisting of an entangled mass of nanotubes having a ‘matted’ appearance, and a micro-scale sample comprising discrete nanotubes aligned between two gold electrodes, 1 μm apart (Fig. 4).

Different excitation wavelengths interact differently with carbon nanotubes, depending on the nanotubes’ size and properties, so Raman spectra were acquired from both samples using 532 nm and 633 nm laser excitation. As a control, the bulk sample was also analysed using a standard Renishaw Raman microscope, employing a research grade optical microscope system and the same RM1000 spectrometer unit and lasers as above: the sample was viewed with white light before switching to the laser beam for Raman analysis. The spatial resolution of the optical microscope proved insufficient to image discrete nanotubes in either the bulk or micro-scale sample.

Results and discussion

Raman spectra from the bulk sample were acquired from inside the SEM chamber, and from the optical microscope system using 532 nm and 633 nm excitation, and confirm that the same spectral resolution is achieved with the SCA (Figs 5a and 6a) as with the optical microscope system (Figs 5b and 6b). The two spectra taken using 633 nm radiation (Fig. 6) were 3 to 4 times more intense than the 532 nm excited spectra (Fig. 5), clearly showing resonance enhancement.

Note: the efficiency of Raman scattering varies approximately with ν^4 , where ν is the frequency of the excitation wavelength. Therefore a two-fold increase in signal intensity would be expected in changing from 532 nm to 633 nm alone, with the remainder of the increase being caused by resonance effects.

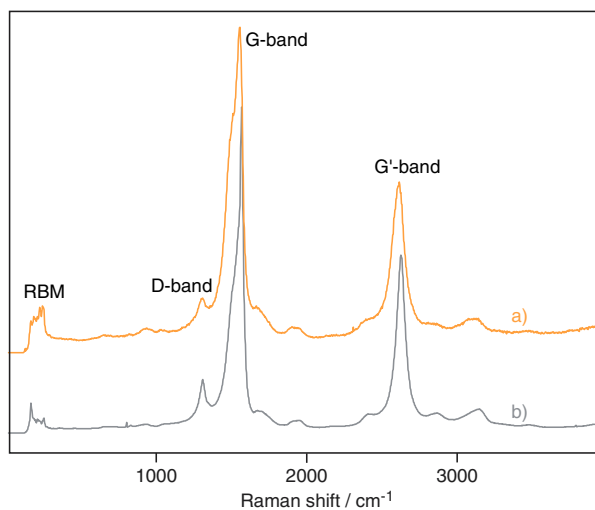


Figure 5
Raman spectra of bulk carbon nanotubes acquired using 532 nm excitation with a) the SCA, and b) conventional sampling under the optical microscope system.

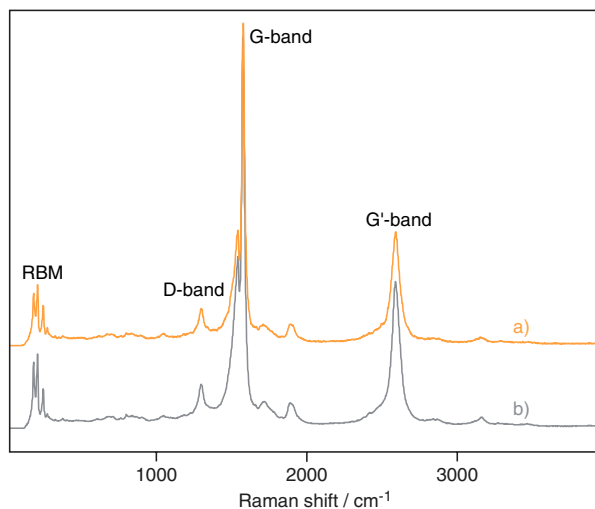


Figure 6
Raman spectra of bulk carbon nanotubes acquired using 633 nm excitation with a) the SCA, and b) conventional sampling under the optical microscope system.

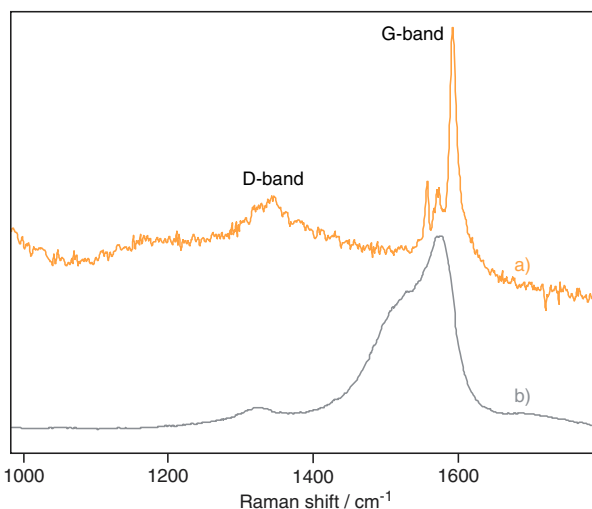


Figure 7
Raman spectra of a) discrete, and b) bulk, carbon nanotube samples, acquired using 532 nm excitation.

To a first approximation, the frequency of the radial breathing mode (RBM) in the Raman spectra of carbon nanotubes depends inversely on the diameter of the tubes,^{6,8} according to the equation,

$$\omega_{RBM} = \alpha/d_t$$

where ω_{RBM} is the frequency of the RBM in cm^{-1} , d_t is the diameter of the nanotubes in nm, and α is a constant, depending on the substrate, and has the value of 248 nm cm^{-1} for silicon.⁸ The spectra indicate tubes of diameter in the range 0.9 nm to 1.3 nm. The more intense 633 nm spectra show three maxima in the RBM region, corresponding to diameters of 1.0 nm (256 cm^{-1}), 1.1 nm (216 cm^{-1}), and 1.3 nm (192 cm^{-1}). Although indicating tube diameter within the same range, the RBM mode in the two 532 nm spectra have different shapes, with the SCA spectrum having a maximum intensity corresponding to a tube diameter of 1.0 nm, and the RM spectrum a diameter of 1.3 nm. This is thought to be because the tubes present do not produce a strong enhancement effect at this wavelength, and because the two spectra are likely to originate from different analysis spots, since it is difficult to relocate the same analysis spot when transferring samples between instruments.

The bulk and micro-scale samples were analysed inside the SEM chamber using the SCA with 532 nm and 633 nm laser excitation. It is readily apparent that the spectrum of the micro-scale nanotubes (Fig 7a) is much sharper than that of the bulk sample (Fig. 7b). This is a result of the low density of the micro-scale sample, presenting only a few resonant nanotubes of well-defined structure and orientation in the laser beam path, yielding well-defined discrete vibrational modes. In bulk samples, there are a range of tube structures and orientations in the laser beam path, making the Raman bands much broader (inhomogeneous broadening).⁹

Raman signal intensities from the micro-scale nanotube sample inside the SEM chamber were lower than those for the bulk, which is expected since there are fewer scattering species in the laser beam path. Although resonance enhancement was observed at 532 nm excitation for this sample, it was insufficient to reveal the RBM. However, since the resonance occurred at a lower wavelength than for the bulk sample, it can be inferred that the micro-scale nanotube sample has a smaller mean diameter than the bulk sample.⁶

Conclusions

This study clearly shows that Raman spectroscopy using the structural and chemical analyser for SEM provides information that is not available using either optical microscope based spectroscopy or SEM in isolation, namely the ability to visualise, analyse, and characterise carbon nanotubes *in situ*.

The SEM-SCA adds a new dimension to the analysis of carbon nanotubes, enabling the nanotube(s) giving rise to the Raman signal to be observed directly in the SEM. According to Prof. Anna Swan, of Boston University, the technology is potentially "really valuable...for one thing, one would see if there is more than one tube in the vicinity that could cause interactions, if there are visible defects or branchings of tubes, or if there are ropes rather than single tubes."⁹

Other nanotechnology applications, such as self-assembling structures will also benefit from this technique: structures too small to be imaged by optical microscopy can be imaged using SEM, and analysed simultaneously using Raman spectroscopy.

Acknowledgements

Renishaw plc wishes to thank:

Prof. R. J. Young of the Materials Science Centre, UMIST/University of Manchester, UK, for supplying the 785 nm excited spectra;

the Chemistry Division of the Naval Research Laboratory, USA, for access to their equipment and provision of the samples;

Prof. A. K. Swan of Boston University, USA, and Prof. R. Hauge of Rice University, USA, for helpful discussions.

References

- 1 S. Iijima, *Nature*, **354**, 56 (1991).
- 2 A. Jorio, A. G. Souza Filho, G. Dresselhaus, M. S. Dresselhaus, A. K. Swan, M. S. Ünlü, B. B. Goldberg, M. A. Pimenta, J. H. Hafner, C. M. Lieber, *Phys. Rev. B*, **65(15)**, 155412 (2002).
- 3 C. A. Cooper, R. J. Young, M. Halsall, *Composites A: Applied Science and Manufacturing*, **32(3-4)**, 401, (2001).
- 4 A. G. Souza Filho, A. Jorio, A. K. Swan, M. S. Ünlü, B. B. Goldberg, R. Saito, J. H. Hafner, C. M. Lieber, M. A. Pimenta, G. Dresselhaus, M. S. Dresselhaus, *Phys. Rev. B*, **65(8)**, 085417 (2002).
- 5 Y. Zhonghous, L. E. Brus, *J. Phys. Chem. A*, **104(47)**, 10995 (2000).
- 6 M. S. Dresselhaus, P. C. Eklund, *Advances in Physics*, **49(6)**, 705 (2000).
- 7 A. R. Bhattacharyya, T. V. Sreekumar, T. Lui, S. Kumar, L. M. Ericson, R. H. Hauge, R. E. Smalley, *Polymer (London)*, **44(8)**, 2373 (2003).
- 8 D. Galkowski, Y. Yumazawa, Y. Maniwa, I. Umezi, S. Suzuki, Y. Ohtsuka, Y. Achiba, *Synthetic Met.*, **103**, 2555 (1999).
- 9 A. K. Swan, *personal communication*.

Renishaw is continually improving its products and reserves the right to change specifications without notice.